Journal of Sound and Vibration (2001) **246**(3), 461–481
doi:10.1006/jsvi.2001.3667, available online at http://www.idealibrary.com on IDEAL®

VIBRATION ANALYSIS OF BEAMS USING THE GENERALIZED DIFFERENTIAL QUADRATURE RULE AND DOMAIN DECOMPOSITION

G. R. LIU AND T. Y. WU

Department of Mechanical Engineering, The National University of Singapore, 10 *Kent Ridge Crescent,* 119260, *Singapore, Singapore. E-mail: engp8773@nus.edu.sg*

(*Received* 15 *June* 2000, *and in final form* 10 *January* 2001)

This study dealt with domain decomposition in the recently proposed generalized differential quadrature rule. In detail, the authors concentrated on the free vibration of multispan and stepped Euler beams, and beams carrying an intermediate or end concentrated mass. Since compatibility conditions should be implemented in a strong form at the junction of the subdomains concerned, the FEM techniques used for internal moments and shear forces must not be used. Compatibility conditions and their differential quadrature expressions were explicitly formulated. A peculiar phenomenon was found in differential quadrature applications that equal–length subdomains gave more accurate results than unequal–length ones using the same number of subdomain grids. Various examples were presented and very accurate results have been obtained.

1. INTRODUCTION

The differential quadrature method (DQM) was first advanced by Bellman and his associates in the early 1970s [1, 2] aiming towards offering an efficient numerical method for solving non-linear partial differential equations. The method has since been applied successfully to various problems. When applied to problems with globally smooth solutions, the DQM can yield highly accurate approximations with relatively few grid points. This has made the DQM a favorable choice in comparison to standard finite difference and finite element methods. In recent years, the DQM has become increasingly popular in solving differential equations and is gradually emerging as a distinct numerical solution technique. An updating of the state of the art on the DQM and a comprehensive survey of its applications are available from two recent review papers [3, 4]. Bellomo [3] focused his attention on the conventional DQM, which dealt with differential equations of no more than second order. Bert and Malik [4] have cited seven examples to explain its applications, six of which still belong to the conventional DQM. Only the third of the seven examples dealt with the high order differential equation of Euler beam, whose governing equation is a fourth order one with double boundary conditions at each boundary. The main difficulty for such high order problems as Euler beams is that there are multiple boundary conditions but only one variable (function value) at each boundary. To apply the double conditions, a δ-point approximation approach of the sampling points was first proposed by Jang *et al.* in 1989 [5] and discussed thoroughly by Bert and Malik [4]. The crux of the δ-point technique is that an inner point near the boundary point is approximately regarded as a boundary point. The introduction of the δ-point technique to multiple boundary condition problems indicated a major development in the application of the DQM to high order differential equations in solid mechanics. However, this breakthrough was also accompanied by a major disadvantage, an arbitrary choice of the δ-value. Shu and Chen [6] made a new endeavor to improve the distribution of the sampling points still using the δ-point technique.

A detailed literature review is unnecessary due to the recent appearance of the two review papers [3, 4]. In order to develop a better alternative to the δ-point technique in solving fourth order differential equations for beam and plate problems, a new method was proposed in references [7–10], where the boundary points' rotation angles of beam and plate structures were employed as independent variables. Therefore, the shortcomings corresponding to the δ-point technique have been overcome successfully. Wang and Gu [7] also mentioned a generalization of their method to sixth and eighth order equations, and Bellomo [3] also tried to generalize the conventional DQM to more than third order equations. However, they [3, 7] did not give the details of the implementation, and no paper related to the just-mentioned generalizations has appeared until the present time to the authors' knowledge.

The generalization of the DQM to any high order differential equations is apparently an urgent need in the present DQM research. The generalized differential quadrature rule (GDQR) has been proposed recently by the present authors [11–17] and detailed formulations have been presented to implement any high order differential equations. The GDQR has been applied for the first time to sixth and eighth order problems [18–20] and to third order problems [20] without using the δ-point technique. Moreover, the GDQR has been extended to high order initial value differential equations of second to fourth orders [12–14], while no one has mentioned this generalization.

In this paper the GDQR was still applied to the Euler beam problem. It is seemingly unnecessary for this kind of simple problem to be dealt with again, since it has been solved in many papers either using the δ-point technique [4, 21] or not [7, 8, 12]. A scrutiny has been made only to find that a beam with intermediate supports has not been coped with in references [7, 8, 12]. Du *et al.* [21] studied Euler beam with an internal pinned support, where Table 2 showed that the critical loads converged to only two or three significant figures even using as many as 23 sampling points. A similar problem, a circular annular plate with an intermediate circular support, was studied in reference [22]. The fundamental frequencies obtained using the DQM differed by about 10% from exact values, and the DQM did not provide satisfactory accuracy for some cases. It is apparent that an error must have occurred in these simple problems. Domain decomposition should have been employed at the intermediate supports but failed to be applied in references [21, 22], because a shear force discontinuity exists there and the continuously differentiable trial functions are employed in the DQM. Domain decomposition has been used and very accurate results have been obtained by the present authors [15]. The above analysis indicates that the study in this paper is necessary for a correct and thorough understanding of the DQ techniques. Moreover, the solution accuracy produced by the method itself can be substantiated quantitatively, since many examples have analytic solutions and the disturbance caused by δ-point values is exempted.

In this paper, the authors concentrated on the free vibration of multispan and stepped Euler beams, and beams carrying an intermediate or end concentrated mass. Since most functions do not have globally smooth solutions, domain decomposition must be employed at the junction of the subdomains concerned. Compatibility conditions and their differential quadrature expressions were explicitly formulated. The length of subdomains was studied in detail. Ample examples were employed to display the application of the domain decomposition in the DQ technique.

2. APPLICATIONS

The free vibration of Euler beams is governed by fourth order differential equations. The fourth order differential equations for various problems have been solved using the GDQR in papers [12, 15–17], and the GDQR expression for a fourth order boundary value differential equation has been used as follows:

$$w^{(r)}(x_i) = \frac{\mathrm{d}^r w(x_i)}{\mathrm{d}x^r} = \sum_{j=1}^{N+2} E_{ij}^{(r)} U_j \quad (i = 1, 2, \ldots, N), \tag{1}$$

where $\{U_1, U_2, \ldots, U_{N+2}\} = \{w_1^{(1)}, w_1, w_2, \ldots, w_{N-1}, w_N^{(1)}, w_N\}$ is employed for the convenience of the notation. w_j is the function of value at point x_j, $w_1^{(1)}$ and $w_N^{(1)}$ are the first order derivatives of the displacement function, i.e.; rotation angles, at the first and Nth points. $E_{ij}^{(r)}$ are the rth order weighting coefficients at point x_i. The GDQR explicit weighting coefficients have been derived in references [12, 17] and were used directly in this paper.

The cosine–type sampling points in normalized interval [0, 1] will be employed in this work. Their advantage has been discussed in paper [4]

$$x_i = \frac{1 - \cos[(i-1)\pi/(N-1)]}{2} \quad (i = 1, 2, \ldots, N). \tag{2}$$

2.1. EXAMPLE 1: STEPPED BEAMS

Consider the free vibration of a straight Euler beam having stepped cross-section only at one place, as shown in Figure 1. These two sections have uniform cross-sections individually. They have different flexural rigidity (EI_1 and EI_2) and different cross-section area (A_1 and A_2). Here the GDQR's solutions are compared with those analytical solutions in paper [23], which considered a stepped beam with circular-section and with

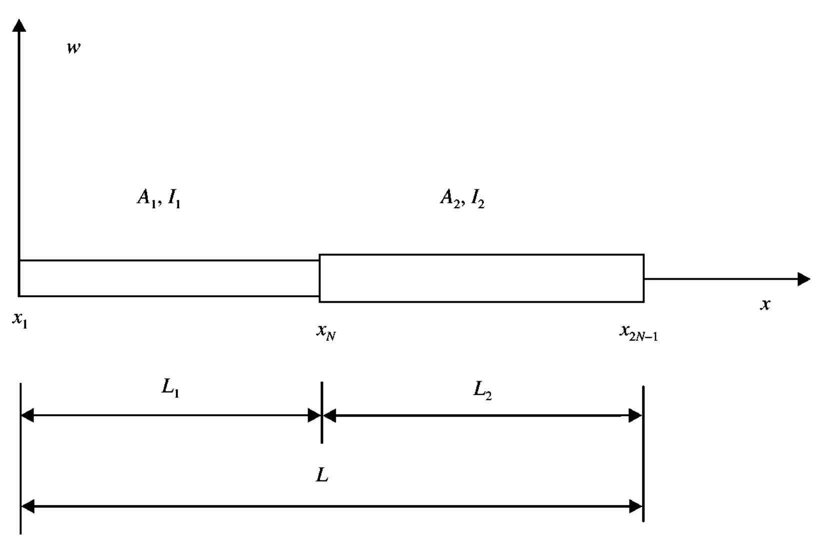

Figure 1. The stepped-beam geometry.

$L_1 = L_2 = L/2$ and $\beta = I_2/I_1$. Then the first and second section's governing differential equations are written, respectively, as follows:

$$EI_1 \frac{d^4 w}{dx^4} = \omega^2 \rho A_1 w, \quad x \subset [0, L_1], \tag{3}$$

$$EI_2 \frac{d^4 w}{dx^4} = \omega^2 \rho A_2 w, \quad x \subset [L_1, L], \tag{4}$$

where ρ is the density, ω the circular frequency, and L the total length of the beam. Through normalization manipulation, equations (3) and (4) are written, respectively, as

$$\left(\frac{L}{L_1}\right)^4 \frac{d^4 w}{d\zeta^4} = \lambda^4 w, \quad \zeta \subset [0, 1], \tag{5}$$

$$\sqrt{\beta}\left(\frac{L}{L_2}\right)^4 \frac{d^4 w}{d\zeta^4} = \lambda^4 w, \quad \zeta \subset [0, 1], \tag{6}$$

where $\lambda = \sqrt[4]{\omega^2 \rho A_1 L^4 / EI_1}$ is dimensionless frequency parameter, and ζ normalized local co-ordinate.

Usually, the same number N of sampling points of subdomains is used. These two sections thus have a total of $2N - 1$ points, as shown in Figure 1. The two sections shared the common point x_N, along with its two corresponding variables w_N and $w_N^{(1)}$. The independent variables of the first section $\{U^{[1]}\}$ and the second section $\{U^{[2]}\}$ in the global co-ordinate are expressed as follows:

$$\{U^{[1]}\} = \{U_1, U_2, \dots, U_{N+2}\} = \{w_1^{(1)}, w_1, w_2, \dots, w_{N-1}, w_N^{(1)}, w_N\}, \tag{7a}$$

$$\{U^{[2]}\} = \{U_{N+1}, U_{N+2}, \dots, U_{2N+2}\} = \{w_N^{(1)}, w_N, w_{N+1}, \dots, w_{2N-2}, w_{2N-1}^{(1)}, w_{2N-1}\}. \tag{7b}$$

The whole beam has a total of $2N + 2$ independent variables as expressed in equation (7). According to equation (1), the GDQR analogues for governing equations (5) and (6) at each section's inner points x_i can be written, respectively, as follows:

$$\left(\frac{L}{L_2}\right)^4 \sum_{j=1}^{N+2} E_{ij}^{(4)} U_j^{[1]} = \lambda^4 w_i \quad (i = 2, 3, \dots, N-1), \tag{8}$$

$$\sqrt{\beta}\left(\frac{L}{L_2}\right)^4 \sum_{j=1}^{N+2} E_{(i-N+1)j}^{(4)} U_{N+j}^{[2]} = \lambda^4 w_i \quad (i = N+1, N+2, \dots, 2N-2). \tag{9}$$

Equations (8) and (9) have a total number of $2 \times (N-2)$ equations. The compatibility conditions at the common points x_N are that: (1) the bending moment calculated by section 1 equals the bending moment computed by section 2, (2) the shear force calculated by section 1 equals the shear force computed by section 2. They are expressed, respectively, as follows:

$$EI_2 \frac{d^2 w}{dx^2} = EI_1 \frac{d^2 w}{dx^2}, \quad EI_2 \frac{d^3 w}{dx^3} = EI_1 \frac{d^3 w}{dx^3}. \tag{10}$$

The two compatibility conditions' GDQR analogues are written, respectively, as

$$\beta\sum_{j=1}^{N+2} E_{1j}^{(2)}U_{N+j}^{[2]} - \sum_{j=1}^{N+2} E_{Nj}^{(2)}U_j^{[1]} = 0, \quad \beta\sum_{j=1}^{N+2} E_{1j}^{(3)}U_{N+j}^{[2]} - \sum_{j=1}^{N+2} E_{Nj}^{(3)}U_j^{[1]} = 0. \tag{11}$$

For simplicity and convenience, the boundary conditions of pinned, clamped, free, and sliding types are denoted as P, C, F and S respectively. The P–C boundary condition will identify the beam with the ends $x = 0$ and L having pinned and clamped boundary conditions respectively. Four types of boundary conditions (pinned, clamped, free and sliding) are considered, respectively, as follows:

$$w = \frac{\mathrm{d}^2w}{\mathrm{d}x^2} = 0, \quad w = \frac{\mathrm{d}w}{\mathrm{d}x} = 0, \quad \frac{\mathrm{d}^2w}{\mathrm{d}x^2} = \frac{\mathrm{d}^3w}{\mathrm{d}x^3} = 0, \quad \frac{\mathrm{d}w}{\mathrm{d}x} = \frac{\mathrm{d}^3w}{\mathrm{d}x^3} = 0. \tag{12–15}$$

The GDQR analogues for equation (12) are written at $x = 0$ and L, respectively,

$$U_2 = 0, \quad \sum_{j=1}^{N+2} E_{1j}^{(2)}U_j^{[1]} = 0 \quad (x = 0), \tag{16a}$$

$$U_{2N+2} = 0, \quad \sum_{j=1}^{N+2} E_{Nj}^{(2)}U_{N+j}^{[2]} = 0 \quad (x = L). \tag{16b}$$

For clamped ends at $x = 0$ and L, one has from equation (13), respectively,

$$U_2 = 0, \quad U_1 = 0 \quad (x = 0), \tag{17a}$$

$$U_{2N+2} = 0, \quad U_{2N+1} = 0 \quad (x = L) \tag{17b}$$

for free ends at $x = 0$ and L and from equation (14),

$$\sum_{j=1}^{N+2} E_{1j}^{(3)}U_j^{[1]} = 0, \quad \sum_{j=1}^{N+2} E_{1j}^{(2)}U_j^{[1]} = 0 \quad (x = 0), \tag{18a}$$

$$\sum_{j=1}^{N+2} E_{Nj}^{(3)}U_{N+j}^{[2]} = 0, \quad \sum_{j=1}^{N+2} E_{Nj}^{(2)}U_{N+j}^{[2]} = 0 \quad (x = L) \tag{18b}$$

and for sliding ends at $x = 0$ and L and from equation (15),

$$U_1 = 0, \quad \sum_{j=1}^{N+2} E_{1j}^{(3)}U_j^{[1]} = 0 \quad (x = 0), \tag{19a}$$

$$U_{2N+1} = 0, \quad \sum_{j=1}^{N+2} E_{Nj}^{(3)}U_{N+j}^{[2]} = 0 \quad (x = L). \tag{19b}$$

There are two boundary conditions at each end, and totally four boundary conditions, which have four GDQR analogues from a proper combination of equations (16)–(19).

TABLE 1

Numerical results for $\lambda = \sqrt[4]{\rho A_1 \omega^2 L^4 / EI_1}$ of the first two modes of stepped beams for various boundary conditions

Mode	I_2/I_1	P–P	C–C	C–F	C–P	F–F
	1	3·14159	4·73004	1·87510	3·92660	4·73004
	5	3·22690	5·09501	1·56120	4·03498	4·91579
1	10	3·14294	5·26125	1·43629	3·93864	4·85241
	20	3·01242	5·50647	1·31977	3·77582	4·74052
	40	2·85253	5·85877	1·21181	3·57074	4·60333
	1	6·28319	7·85320	4·69409	7·06858	7·85320
	5	7·11734	8·84035	4·72584	7·97403	8·83221
2	10	7·48932	9·23935	4·59285	8·48705	9·21336
	20	7·75541	9·49788	4·40079	8·95134	9·44771
	40	7·89647	9·62033	4·16961	9·26478	9·54664
		S–S	S–P	C–S	F–S	F–P
	1	3·14159	1·57080	2·36502	2·36502	3·92660
	5	3·67592	1·56116	2·38563	3·05981	4·31396
1	10	3·98830	1·52619	2·37320	3·32444	4·33175
	20	4·27725	1·47787	2·31459	3·52235	4·28989
	40	4·49393	1·41851	2·21163	3·64619	4·21638
	1	6·28319	4·71239	5·49780	5·49780	7·06858
	5	6·70841	5·18341	5·91362	5·92170	7·94119
2	10	6·85899	5·25357	6·17931	6·16921	8·44328
	20	7·09381	5·24429	6·56198	6·53542	8·89891
	40	7·47091	5·18642	7·06626	7·03141	9·20636

Together with two equations from compatibility condition equation (11) and $2 \times (N-2)$ equations from governing equations (8) and (9), a total number of $2N + 2$ equations is formed. The total number of independent variables expressed in equation (7) is also $2N + 2$. The resulting differential quadrature equations can be solved to get the required frequencies. The procedures in the solution of formed algebraic eigenvalue equations are detailed in references [4, 12, 15] and omitted here for brevity. These four types of boundary conditions will form 10 combinations of beam boundary conditions. The present work calculated all the 10 cases with different β values and listed the results in Table 1. Using eight sampling points for each subdomain, the GDQR fundamental frequencies for all the 10 cases are exactly the same as the exact analytical solutions in reference [23] and are accurate to five significant figures. Since only fundamental frequencies were given in reference [23], the second frequencies are calculated purposely for a comparison with other methods. Twelve points are needed for the second frequencies to be accurate to five significant figures.

2.2. EXAMPLE 2: UNIFORM MULTISPAN BEAMS

Consider the equi-spaced uniform multispan beams with each span length l, total length L, flexural rigidity EI and cross-section A. Other prerequisites are the same as those in example 1. The multispan beam with pinned intermediate supports would have a concentrated shear force at the inner supports, which also constitute another kind of discontinuity. Therefore, domain decomposition must be employed there. What compatibility conditions does one have at this discontinuous place? The rotation angle and the concentrated force are unknown and thus cannot form a compatibility condition. The zero displacement is certainly the simplest compatibility condition. The second compatibility condition is that the bending moment calculated by the left section equals the bending moment computed by the right section. Here a double-span uniform beam's compatibility conditions and corresponding GDQR analogues are given as an example:

$$w_N = 0 \quad \left(EI\,\frac{\mathrm{d}^2 w}{\mathrm{d}x^2}\right)_{left} = \left(EI\,\frac{\mathrm{d}^2 w}{\mathrm{d}x^2}\right)_{right}, \tag{20}$$

$$U_{N+2} = 0, \quad \sum_{j=1}^{N+2} E_{Nj}^{(2)} U_j^{[1]} - \sum_{j=1}^{N+2} E_{1j}^{(2)} U_{N+j}^{[2]} = 0. \tag{21}$$

More span beam's identical compatibility conditions at other junctions can be obtained in a similar way and omitted here for simplicity. The GDQR analogues of 10 combinations of boundary conditions have already been listed in equations (16)–(19) for double-span beams. Similar expressions can be easily obtained for more span beams. The governing equation of the $(m + 1)$th span and its GDQR analogues can be written, respectively, as follows:

$$EI\,\frac{\mathrm{d}^4 w}{\mathrm{d}x^4} = \omega^2 \rho A w, \quad x \subset [ml, (m+1)l], \tag{22}$$

$$\sum_{j=1}^{N+2} E_{(i-Q+1)j}^{(4)} U_{P+j}^{[m+1]} = \lambda^4 w_i \quad (i = Q+1, Q+2, \ldots, Q+N-2), \tag{23}$$

where $\lambda = \sqrt[4]{\omega^2 \rho A l^4 / EI}$ is a dimensionless frequency parameter. $Q = mN - m + 1$ is the numbering of the first sampling point of the $(m + 1)$th span, and $P = m(N + 2) - 2m + 1$ is the numbering of the last variable of the mth span at inner points.

Again all the 10 combinations of boundary conditions are calculated and compared with results in reference [24], which listed the first six frequencies for 1–15 spans. The finite element method was used to obtain the frequencies in reference [24]. The present GDQR's first–sixth frequencies are all accurate to more than three significant figures. Here, only F–F case is listed in Table 2 for a comparison. The other cases are also calculated but omitted for simplicity. For a comparison with other methods, the seventh frequencies are also calculated on purpose.

2.3. EXAMPLE 3: UNIFORM BEAMS WITH END MASS

Reference [25] calculated the free vibration of an S–C single–span beam carrying a concentrated mass M at the sliding end. More accurate results than those in reference [25] are presented here. Since the mass is at the end and the beam is of uniform single span, domain decomposition is unnecessary here. This example is designed to show how to implement the boundary condition with the frequency in it. The two boundary conditions

TABLE 2

Frequency parameters $\lambda = \sqrt[4]{\rho A \omega^2 l^4 / EI}$ *for F–F multispan beam*

Method	N	Span no.	Mode sequence 1	2	3	4	5	6	7
GDQR	20	2	1·87510	3·92660	4·69409	7·06858	7·85476	10·21018	10·99554
	15	3	1·41181	1·64778	3·57994	4·27231	4·70627	6·70658	7·43063
	12	4	1·50592	1·57080	3·41310	3·92660	4·43727	4·71239	6·54456
	12	5	1·52987	1·54793	3·32299	3·71010	4·14305	4·52700	4·71607
	10	6	1·53642	1·54145	3·27008	3·56846	3·92660	4·28449	4·58076
	9	7	1·53823	1·53964	3·23687	3·47167	3·76940	4·08379	4·38121
	9	8	1·53874	1·53913	3·21483	3·40317	3·65284	3·92660	4·20035
	9	9	1·53888	1·53899	3·19954	3·35325	3·56450	3·80325	4·04995
	9	10	1·53892	1·53895	3·18854	3·31594	3·49625	3·70533	3·92660
	9	11	1·53893	1·53894	3·18036	3·28743	3·44263	3·62658	3·82513
	9	12	1·53893	1·53894	3·17414	3·26523	3·39985	3·56250	3·74103
	9	13	1·53894	1·53894	3·16929	3·24763	3·36529	3·50978	3·67075
	9	14	1·53894	1·53894	3·16545	3·23348	3·33701	3·46597	3·61155
	9	15	1·53894	1·53894	3·16235	3·22194	3·31362	3·42925	3·56129
	9	16	1·53894	1·53894	3·15981	3·21241	3·29409	3·39820	3·51834
	9	17	1·53894	1·53894	3·15771	3·20447	3·27763	3·37175	3·48139
	9	18	1·53894	1·53894	3·15596	3·19777	3·26365	3·34907	3·44940
	9	19	1·53894	1·53894	3·15447	3·19208	3·25167	3·32948	3·42156
	9	20	1·53894	1·53894	3·15320	3·18721	3·24134	3·31247	3·39720
Reference [24]		2	1·875	3·927	4·694	7·069	7·855	10·21	
		3	1·412	1·648	3·580	4·273	4·707	6·707	
		4	1·506	1·571	3·413	3·928	4·438	4·713	
		5	1·530	1·548	3·324	3·710	4·144	4·528	
		6	1·537	1·542	3·270	3·568	3·927	4·285	
		7	1·538	1·540	3·237	3·471	3·770	4·084	
		8	1·539	1·539	3·215	3·404	3·653	3·926	
		9	1·539	1·539	3·200	3·353	3·564	3·803	
		10	1·539	1·539	3·189	3·316	3·496	3·705	
		11	1·539	1·539	3·180	3·287	3·443	3·626	
		12	1·539	1·539	3·174	3·265	3·400	3·563	
		13	1·539	1·539	3·169	3·248	3·365	3·510	
		14	1·539	1·539	3·166	3·234	3·337	3·466	
		15	1·539	1·539	3·162	3·222	3·313	3·430	

at sliding end are zero rotation angle and the following equation [25]:

$$EI\,\frac{\mathrm{d}^3W(x_1,t)}{\mathrm{d}x^3}=M\,\frac{\partial^2W(x_1,t)}{\partial t^2}. \tag{24}$$

The clamped boundary condition is identical to the above-mentioned one. The GDQR analogue of governing equation is identical to equation (8) with $L_1=L$. If the normal mode is assumed as $W(x,t)=w(x)\mathrm{e}^{\mathrm{i}\omega t}$, substituting into equation (24) produces

$$EI\,\frac{\mathrm{d}^3w(x_1)}{\mathrm{d}x^3}=-\,M\omega^2w_1\,. \tag{25}$$

Its GDQR analogue can be written as

$$-\frac{\rho AL}{M}\sum_{j=1}^{N+2}E_{1j}^{(3)}U_j=\lambda^4w_1, \tag{26}$$

where $\lambda=\sqrt[4]{\omega^2\rho AL^4/EI}$ is dimensionless frequency parameter.

This boundary condition contains the eigenvalue of the problem. Usually, the two displacements and two rotation angles at two ends can be eliminated in the final standard eigenvalue equation of order $N-2$, as shown in papers [4, 12]. But now one boundary displacement w_1 is connected with the frequency. Then the final standard eigenvalue equation is of order $N-1$. Even if all the boundary independent variables are connected with the frequency, with the final standard eigenvalue equation being of order $N+2$, no algorithmic difficulty is caused in the GDQR. The analytic frequency characteristic equation was [25]

$$\frac{M}{\rho AL}=\frac{\sin\lambda\cosh\lambda+\cos\lambda\sinh\lambda}{\lambda(1-\cos\lambda\cosh\lambda)}. \tag{27}$$

Similarly, if the beam is an F–C single-span beam carrying a concentrated mass at the free end, only the boundary condition at $x=0$ is changed from zero rotation angle to zero moment with all the other equations identical to those for the S–C case. Table 3 showed the GDQR results. The characteristic equation for the F–C case was [26]

$$\frac{M}{\rho AL}=\frac{1+\cos\lambda\cosh\lambda}{\lambda(\sin\lambda\cosh\lambda-\cos\lambda\sinh\lambda)}. \tag{28}$$

2.4. EXAMPLE 4: STEPPED BEAMS WITH END MASS

For the above-mentioned S–C single-span beam carrying a concentrated mass at the sliding end, reference [27] has considered non-uniform cross-section with discontinuity at $x=L/3$, $L/2$ and $2L/3$, as shown in Figure 2. Each section has the same width of a rectangular cross-section, and their height ratio $\alpha=t_1/t_2=0{\cdot}8$. The GDQR results for $x=L/2$ case are obtained with two sections. The GDQR results for $x=L/3$ and $2L/3$ cases are obtained with three equal-length sections. All the necessary boundary conditions,

TABLE 3

Frequency parameter $\lambda = \sqrt[4]{\rho A \omega^2 L^4 / EI}$ *of uniform beams with end mass*

Boundary condition	$M / \rho AL$	Mode sequence 1	2	3	4	5	6	7
S–C	0	2·36501	5·49778	8·63934	11·78091	14·92249	18·06407	21·20564
	0·2	2·13339	5·17434	8·21537	11·29334	14·38954	17·49745	20·61314
	0·6	1·87254	4·96859	8·02377	11·12516	14·24155	17·36611	20·49541
	1	1·71888	4·89277	7·96446	11·07821	14·20285	17·33325	20·46690
	1·6	1·57028	4·84017	7·92627	11·04909	14·17936	17·31359	20·45000
	2	1·49954	4·82063	7·91266	11·03891	14·17123	17·30683	20·44422
	2·6	1·41742	4·80159	7·89967	11·02929	14·16360	17·30050	20·43882
	3	1·37341	4·79279	7·89376	11·02494	14·16016	17·29766	20·43640
	3·6	1·31834	4·78302	7·88726	11·02019	14·15641	17·29457	20·43376
	4	1·28711	4·77804	7·88398	11·01779	14·15452	17·29301	20·43244
	4·6	1·24639	4·77210	7·88009	11·01496	14·15229	17·29118	20·43088
	5	1·22252	4·76890	7·87800	11·01344	14·15110	17·29019	20·43005
	10	1·03713	4·74995	7·86578	11·00461	14·14419	17·28451	20·42522
	15	0·93997	4·74342	7·86163	11·00163	14·14186	17·28260	20·42361
	20	0·87607	4·74012	7·85954	11·00013	14·14069	17·28164	20·42279
F–C	0	1·87509	4·69404	7·85468	10·99543	14·13703	17·27859	20·42015
	0·5	1·41996	4·11113	7·19034	10·29845	13·42100	16·55028	19·68326
	1	1·24792	4·03114	7·13413	10·25662	13·38776	16·52273	19·65975
	1·5	1·14644	3·99951	7·11342	10·24168	13·37608	16·51315	19·65163
	2	1·07620	3·98257	7·10265	10·23402	13·37012	16·50828	19·64752
	2·5	1·02327	3·97202	7·09605	10·22935	13·36651	16·50533	19·64503
	3	0·98123	3·96482	7·09160	10·22621	13·36409	16·50336	19·64337
	3·5	0·94662	3·95958	7·08838	10·22395	13·36235	16·50194	19·64217
	4	0·91736	3·95561	7·08596	10·22225	13·36104	16·50088	19·64128
	4·5	0·89213	3·95249	7·08406	10·22093	13·36002	16·50005	19·64058
	5	0·87002	3·94998	7·08254	10·21986	13·35920	16·49939	19·64002
	7·5	0·78914	3·94234	7·07794	10·21666	13·35674	16·49739	19·63834
	10	0·73578	3·93847	7·07562	10·21505	13·35550	16·49638	19·63749
	20	0·62051	3·93258	7·07211	10·21262	13·35364	16·49487	19·63623
	50	0·49434	3·92900	7·07000	10·21115	13·35242	16·49397	19·73546
	100	0·41593	3·92780	7·06929	10·21067	13·35214	16·49366	19·63521
	200	0·34986	3·92720	7·06894	10·21042	13·35196	16·49351	19·63508

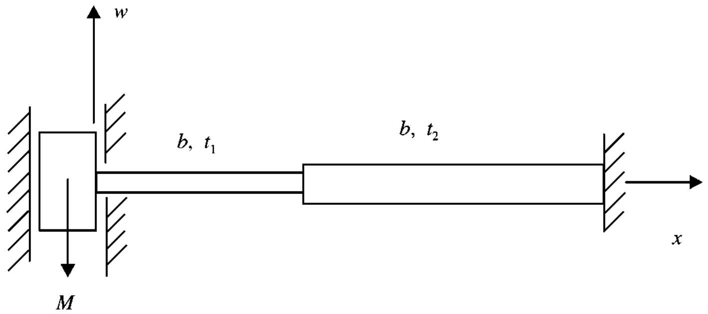

Figure 2. The non-uniform S–C beam with end mass.

compatibility conditions and governing equation have been given before and omitted here for brevity. Table 4 showed good agreements between the GDQRs and FEMs results.

2.5. EXAMPLE 5: UNIFORM BEAMS WITH INTERMEDIATE MASS

References [28, 29] considered the concentrated mass at an intermediate point ($x = L/3$ or $L/2$) of single-span uniform beam. The mass will apply a dynamic concentrated force in vibration problems. Domain decomposition must also be employed, though the beam is uniform single span. For the case $x = L/2$, two equal-length sections are used. The compatibility conditions are as follows:

$$\left(EI\frac{\mathrm{d}^2 w}{\mathrm{d}x^2}\right)_1 = \left(EI\frac{\mathrm{d}^2 w}{\mathrm{d}x^2}\right)_2, \quad \left(EI\frac{\mathrm{d}^3 w}{\mathrm{d}x^3}\right)_2 - \left(EI\frac{\mathrm{d}^3 w}{\mathrm{d}x^3}\right)_1 = M\omega^2 w, \tag{29}$$

where the suffix expresses the section number. The two compatibility conditions' GDQR expressions are written as

$$\left(\frac{L}{L_1}\right)^2 \sum_{j=1}^{N+2} E_{Nj}^{(2)} U_j^{[1]} - \left(\frac{L}{L_2}\right)^2 \sum_{j=1}^{N+2} E_{1j}^{(2)} U_{N+j}^{[2]} = 0,$$

$$\frac{\rho A L}{M}\left(\left(\frac{L}{L_2}\right)^3 \sum_{j=1}^{N+2} E_{1j}^{(3)} U_{N+j}^{[2]} - \left(\frac{L}{L_1}\right)^3 \sum_{j=1}^{N+2} E_{Nj}^{(3)} U_j^{[1]}\right) = \lambda^4 w_N, \tag{30}$$

where $\lambda = \sqrt[4]{\omega^2 \rho A L^4/EI}$ is dimensionless frequency parameter.

The GDQR analogues of governing equations are identical to equations (8) and (9) with $\beta = 1$ (due to uniform cross-section). Only P–P and C–C beams are considered here. For the case $x = L/3$, both three equal-length and two different-length sections are used. The results are listed in Table 5(a)–(c). The FEM was used in paper [24]. The Laplace transform was employed to obtain a characteristic equation in paper [28]. An analytic characteristic equation was obtained in paper [29].

TABLE 4

Frequency parameter $\lambda = \sqrt[4]{\rho A_1 \omega^2 L^4 / EI_1}$ *of S–C stepped* ($x = L/3$, $L/2$, $2L/3$) *and uniform* ($x = 0$) *beams with end mass*

x	Method	$M/\rho A_1 L$							
		0	0·2	0·4	0·6	0·8	1	5	10
0	GDQR	5·59327	4·55135	3·92932	3·50640	3·19544	2·95455	1·49456	1·07564
	Exact [27]	5·59332	4·552	3·929	3·506	3·195	2·954	1·494	1·075
$L/3$	GDQR	6·70986	5·46382	4·71752	4·20968	3·83617	3·54681	1·79350	1·29067
	FEM [27]	6·70	5·45	4·71	4·20	3·83	3·54	1·79	1·28
$L/2$	GDQR	6·82247	5·52233	4·75325	4·23365	3·85322	3·55943	1·79294	1·28945
	FEM [27]	6·81	5·51	4·74	4·22	3·84	3·55	1·79	1·28
$2L/3$	GDQR	6·79785	5·47275	4·69859	4·17885	3·79975	3·50773	1·76203	1·26666
	FEM [27]	6·79	5·46	4·69	4·17	3·79	3·50	1·76	1·26

TABLE 5 (a)

Frequency parameter $\lambda = \sqrt[4]{\rho A \omega^2 L^4 / EI}$ *of uniform beams carrying a concentrated mass at* $x = L/2$

Boundary condition	$\frac{M}{\rho AL}$	Mode sequence					
		1	2	3	4	5	6
	10^{-10}	3·14159	6·28319	9·42478	12·56637	15·70796	18·84956
	10^{-5}	3·14158	6·28319	9·42473	12·56637	15·70788	18·84956
	0·01	3·12607	6·28319	9·37897	12·56637	15·63277	18·84956
	0·01	(3·129)	(6·285)	(9·380)			
	0·1	3·00130	6·28319	9·05955	12·56637	15·17126	18·84956
	0·1	(3·004)	(6·285)	(9·061)			
	0·2	2·88726	6·28319	8·83030	12·56637	14·90092	18·84956
	0·2	{2·887}					
P–P	0·5	2·63931	6·28319	8·47440	12·56637	14·56167	18·84956
	1	2·38319	6·28319	8·23944	12·56637	14·38016	18·84956
	1	{2·384}					
	2	2·09598	6·28319	8·07304	12·56637	14·26797	18·84956
	5	1·71985	6·28319	7·94909	12·56637	14·19198	18·84956
	5	{1·719}					
	10	1·46271	6·28319	7·90264	12·56637	14·16501	18·84956
	10	{1·463}					
	50	0·98746	6·28319	7·86334	12·56637	14·14281	18·84956
	100	0·83135	6·28319	7·85829	12·56637	14·13999	18·84956
	10^{-10}	4·73004	7·85320	10·99561	14·13717	17·27876	20·42035
	10^{-5}	4·73001	7·85320	10·99555	14·13717	17·27867	20·42035
	0·01	4·70065	7·85320	10·94300	14·13717	17·19633	20·42035
	0·01	(4·701)	(7·853)	(10·943)			
	0·1	4·46984	7·85320	10·58876	14·13717	16·70539	20·42035
	0·1	(4·470)	(7·853)	(10·589)			
	0·2	4·26678	7·85320	10·34868	14·13717	16·43074	20·42035
	0·2	{4·250}					

TABLE 5 (a)

Continued

Boundary condition	$\frac{M}{\rho AL}$	Mode sequence 1	2	3	4	5	6
C–C	0·5	3·84707	7·85320	9·99991	14·13717	16·09984	20·42035
	1	3·43776	7·85320	9·78554	14·13717	15·92892	20·42035
	1	{3·440}					
	2	2·99908	7·85320	9·64127	14·13717	15·82532	20·42035
	5	2·44504	7·85320	9·53780	14·13717	15·75599	20·42035
	5	{2·446}					
	10	2·07425	7·85320	9·49990	14·13717	15·73155	20·42035
	10	{2·072}					
	50	1·39727	7·85320	9·46820	14·13717	15·71150	20·42035
	100	1·17604	7·85320	9·46415	14·13717	15·70896	20·42035

Note: Data in "( )" from reference [28], in "{ }" from reference [24].

TABLE 5 (b)

Frequency parameter $\lambda = \sqrt[4]{\rho A \omega^2 L^4 / EI}$, *which is obtained using three equal-length sections, of uniform beams carrying a concentrated mass at* $x = L/3$

Boundary condition	$\frac{M}{\rho AL}$	Mode sequence 1	2	3	4	5	6
	10^{-10}	3·14159	6·28319	9·42478	12·56637	15·70796	18·84956
	10^{-5}	3·14158	6·28316	9·42478	12·56632	15·70790	18·84956
	0·01	3·12991	6·26017	9·42478	12·52046	15·65212	18·84956
	0·01	(3·133)	(6·262)	(9·426)			
	0·1	3·03278	6·09308	9·42478	12·19934	15·33373	18·84956
	0·1	(3·0339)	(6·095)	(9·426)			
	0·2	2·93929	5·96510	9·42478	11·97435	15·16707	18·84956
	0·2	{2·9413}					
P–P	0·5	2·72241	5·75135	9·42478	11·64505	14·97854	18·84956
	0·5	{2·7258}					
	1	2·48255	5·59983	9·42478	11·44416	14·88676	18·84956
	1	{2·485}					
	2	2·19986	5·48777	9·42478	11·31035	14·83304	18·84956
	2	{2·2043}					
	5	1·81570	5·40203	9·42478	11·21524	14·79791	18·84956
	5	{1·8199}					
	10	1·54770	5·36948	9·42478	11·18059	14·78568	18·84956
	10	{1·5514}					
	50	1·04684	5·34178	9·42478	11·15170	14·77571	18·84956
	50	{1·0494}					
	100	0·88156	5·33821	9·42478	11·14802	14·77445	18·84956
	100	{0·88369}					

TABLE 5 (b)

Continued

Boundary condition	$M/\rho AL$	Mode sequence 1	2	3	4	5	6
	10^{-10}	4·73004	7·85320	10·99561	14·13717	17·27876	20·42035
	10^{-5}	4·73002	7·85316	10·99560	14·13713	17·27868	20·42035
	0·01	4·71210	7·81391	10·99152	14·10336	17·20276	20·41394
	0·01	(4·712)	(7·814)	(10·992)			
	0·1	4·56043	7·53842	10·96400	13·86852	16·77405	20·37802
	0·1	(4·560)	(7·538)	(10·964)			
	0·2	4·41153	7·34045	10·94524	13·70666	16·55492	20·35909
C–C	0·5	4·06264	7·03852	10·91762	13·47612	16·31369	20·33683
	1	3·68039	6·84806	10·90034	13·34025	16·19944	20·32541
	1	{3·680}					
	2	3·24028	6·72025	10·88854	13·25206	16·13371	20·31849
	5	2·65859	6·62992	10·87999	13·19058	16·09120	20·31384
	10	2·26054	6·59728	10·87684	13·16843	16·07649	20·31220
	50	1·52559	6·57020	10·87420	13·15008	16·06453	20·31085
	100	1·28435	6·56676	10·87386	13·14774	16·06302	20·31068

Note: Data in "( )" from reference [28], in "{ }" from reference [29].

Table 5 (c)

Frequency parameter $\lambda = \sqrt[4]{\rho A \omega^2 L^4 / EI}$, which is obtained using two sections of different length, of uniform beams carrying a concentrated mass at $x = L/3$

Boundary condition	$\frac{M}{\rho AL}$	Mode sequence					
		1	2	3	4	5	6
	10^{-10}	2·99811	6·42423	9·42478	12·42563	15·84870	18·84956
	10^{-5}	2·99810	6·42421	9·42478	12·42558	15·84864	18·84956
	0·01	2·98631	6·40288	9·42478	12·37620	15·79745	18·84956
	0·01	4·58%	−2·28%	0%	1·15%	−0·90%	0%
	0·1	2·88892	6·24725	9·42478	12·03635	15·50192	18·84956
P–P	0·2	2·79625	6·12734	9·42478	11·80293	15·34420	18·84956
	0·5	2·58429	5·92549	9·42478	11·46580	15·16222	18·84956
	1	2·35306	5·78091	9·42478	11·26193	15·07192	18·84956
	2	2·08297	5·67293	9·42478	11·12669	15·01847	18·84956
	5	1·71801	5·58956	9·42478	11·03079	14·98325	18·84956
	10	1·46407	5·55769	9·42478	10·99589	14·97094	18·84956
	10	5·40%	−3·51%	0%	1·65%	−1·25%	0%
	50	0·99008	5·53048	9·42478	10·96681	14·96088	18·84956
	100	0·83375	5·52697	9·42478	10·96310	14·95961	18·84956
	10^{-10}	4·62970	7·94594	11·07899	13·96678	17·35779	20·50815
	10^{-5}	4·62968	7·94591	11·07899	13·96674	17·35771	20·50814
	0·01	4·61025	7·90999	11·07702	13·92588	17·28748	20·50522
	0·01	2·16%	−1·23%	−0·78%	−0·41%	−0·49%	−0·45%
	0·1	4·44831	7·65829	11·06337	13·64767	16·89121	20·48812

TABLE 5 (c)

Continued

Boundary condition	M / ρAL	Mode sequence 1	2	3	4	5	6
C–C	0·2	4·29298	7·47747	11·05367	13·46121	16·68794	20·47855
	0·5	3·93887	7·20049	11·03871	13·20130	16·46219	20·46673
	1	3·56032	7·02374	11·02889	13·05048	16·35401	20·46040
	2	3·13041	6·90343	11·02197	12·95332	16·29124	20·45647
	5	2·56639	6·81720	11·01684	12·88587	16·25041	20·45379
	10	2·18160	6·78573	11·01492	12·86163	16·23624	20·45283
	10	3·49%	−2·86%	−1·27%	2·33%	−0·99%	−0·69%
	50	1·47204	6·75950	11·01330	12·84155	16·22470	20·45204
	100	1·23925	6·75615	11·01310	12·83900	16·22324	20·45194

Note: Data expressed in per cent are relative errors compared with the results in Table 5(b).

3. DISCUSSION

Domain decomposition must be employed in the DQ technique if the solution function is not continuously differentiable in the solution domain, since the weighting coefficients are obtained using continuously differentiable trial functions. Within a subdomain, the solution function should be continuously differentiable. At the junction of the subdomains concerned, compatibility conditions must be implemented in a strong form. Naturally, the governing equations are written individually for the sections with different flexural rigidity as done in equations (3) and (4), and domain decomposition is applied accordingly. However, domain decomposition should still be employed for multispan beams with uniform cross-sections, since a discontinuity exists there too. Similarly, domain decomposition must be applied to example 5, which is more deceptive since it is a uniform single-span beam. It is clear that every subdomain end has two compatibility conditions corresponding to two independent variables. Four conditions are indispensable to the fourth order governing equations.

In all the examples in this work, eight sampling points for each subdomain produce the fundamental frequencies accurate to about five significant figures. More than 15 discrete points for each subdomain will bring about the first–sixth frequencies accurate to about seven significant figures. For more than five span beams, eight sampling points for each subdomain are usually used.

When the domain decomposition point in examples 4 and 5 is not at the center of the beam (i.e., $x = L/3$ and $2L/3$), three equal-length sections had to be used to obtain more accurate results than two unequal-length sections. In fact, the results obtained using two unequal-length sections are very bad, as shown in Table 5(c) where some relative errors are about 5%. This quite peculiar phenomenon is first reported here in the DQ solution, and needs more study. The FDM and the present DQ technique solve different equations in a strong form. It is well known that the FDM usually produces a worse accuracy with unequal length grids than with equal grids, while the authors think that a similar phenomenon may exist in the present DQ technique.

When the concentrated mass ratio $M/\rho AL$ is gradually reduced to zero, the obtained frequency should equal that calculated without mass. In actual calculation, only a very small number can be employed. The mass ratio $M/\rho AL$ should be larger than 10^{-12}. If it is less than this number, unreasonable results are obtained.

It is interesting to note that the frequencies of the first and second modes for multispan F–F beams in Table 2 are identical (1·53894) when the span number is larger than 11. For multispan F–P, F–C, and F–S beams, their first frequencies are all 1·53894 when the span number exceeds a certain number. The beam should adopt two different modes for the first and second modes. The two different modes for the first and second modes of multispan F–F beams should be exactly the first mode of multispan F–P, F–C, or F–S beams. Therefore, the frequencies of the first and second modes are identical (1·53894) for F–F multispan beams when the span number is larger than 11.

It is also noted that the frequencies for even modes given in Table 5(a) do not change with the change of $M/\rho AL$. The reason is that the displacement at $x = L/2$ is always zero for even modes. The mid-point equals a simply supported point. Therefore, the mid-point mass has no effects, and the corresponding frequencies do not change with the change of $M/\rho AL$.

4. CONCLUSION

Five examples for the free vibration of Euler beams have been applied using the domain decomposition and the GDQR. Since compatibility conditions should be implemented in a strong form at the junction of the subdomains concerned, compatibility conditions and their differential quadrature expressions were explicitly formulated. A peculiar phenomenon was found in the differential quadrature applications that equal-length subdomains give more accurate results than unequal-length ones using the same number of subdomain grids. The study in this work is necessary for a correct and thorough understanding of the DQ techniques. Various examples were presented and very accurate results have been obtained.

REFERENCES

1. R. BELLMAN and J. CASTI 1971 *Journal of Mathematical Analysis and Applications* **34**, 235–238. Differential quadrature and long term integration.
2. R. BELLMAN, B. G. KASHEF and J. CASTI 1972 *Journal of Computational Physics* **10**, 40–52. Differential quadrature: a technique for the rapid solution of non-linear partial differential equations.
3. N. BELLOMO 1997 *Mathematical and Computer Modelling* **26**, 13–34. Nonlinear models and problems in applied sciences from differential quadrature to generalized collocation methods.
4. C. W. BERT and M. MALIK 1996 *Applied Mechanics Review* **49**, 1–27. Differential quadrature method in computational mechanics: a review.
5. S. K. JANG, C. W. BERT and A. G. STRIZ 1989 *International Journal for Numerical Methods in Engineering* **28**, 561–577. Application of differential quadrature to static analysis of structural components.
6. C. SHU and W. CHEN 1999 *Journal of Sound Vibration* **222**, 239–257. On optimal selection of interior points for applying discretized boundary conditions in DQ vibration analysis of beams and plates.
7. X. WANG and H. GU 1997 *International Journal for Numerical Methods in Engineering* **40**, 759–772. Static analysis of frame structures by the differential quadrature element method.
8. W. CHEN, A. G. STRIZ and C. W. BERT 1997 *International Journal for Numerical Methods in Engineering* **40**, 1941–1956. A new approach to the differential quadrature method for fourth-order equations.
9. X. WANG, Y. L. WANG and R. B. CHEN 1998 *Communications in Numerical Methods in Engineering* **14**, 1133–1141. Static and free vibrational analysis of rectangular plates by the differential quadrature element method.
10. H. Z. GU and X. W. WANG 1997 *Journal of Sound Vibration* **202**, 452–459. On the free vibration analysis of circular plates with stepped thickness over a concentric region by the differential quadrature element method.
11. T. Y. WU and G. R. LIU 2000 *in the Abstract Book for ICTAM*2000, 119. 20*th International Congress of Theoretical and Applied Mechanics*, *Chicago*. A generalization of the differential quadrature method.
12. T. Y. WU and G. R. LIU 1999 *Computational Mechanics* **24**, 197–205. The differential quadrature as a numerical method to solve the differential equation.
13. T. Y. WU and G. R. LIU 2000 *Journal of Sound Vibration* **233**, 195–213. The generalized differential quadrature rule for initial-value differential equations.
14. G. R. LIU and T. Y. WU 2000 *Journal of Sound Vibration* **237**, 805–817. Numerical solution for differential equations of a Duffing type nonlinearity using the generalized differential quadrature rule.
15. T. Y. WU and G. R. LIU 2000 *International Journal of Pressure Vessels and Piping* **77**, 149–157. Axisymmetric bending solution of shells of revolution by the generalized differential quadrature rule.
16. T. Y. WU and G. R. LIU 1999 in *Computational Mechanics for the Next Millennium. Proceedings of Fourth Asia–Pacific Conference on Computational Mechanics* (C. M. Wang, K. H. Lee and K. K. Ang, editors), Vol. 1, 223–228. A generalized differential quadrature rule for analysis of thin cylindrical shells.
17. T. Y. WU and G. R. LIU 2001 *International Journal for Numerical Methods in Engineering* **50**, 1907–1929. The generalized differential quadrature rule for fourth order differential equations.
18. T. Y. WU and G. R. LIU 2000 *Communications in Numerical Methods in Engineering* **16**, 777–784. Application of the generalized differential quadrature rule to sixth-order differential equations.

19. T. Y. WU and G. R. LIU 2001 *Communications in Numerical Methods in Engineering* **17**, 355–364. Application of the generalized differential quadrature rule to eighth-order differential equations.
20. G. R. LIU and T. Y. WU 2000 *International Journal for Numerical Methods in Engineering* (in press). An application of the generalized differential quadrature rule in Blasius and Onsager equations.
21. H. DU, K. M. LIEW and M. K. LIM 1996 *Journal of Engineering Mechanics*, *American Society of Civil Engineers* **122**, 95–100. Generalized differential quadrature method for buckling analysis.
22. E. ROMANELLI, R. E. ROSSI, P. A. A. LAURA and R. H. GUTIERREZ 1998 *Journal of Sound Vibration* **212**, 564–571. Transverse vibrations of a circular annular plate with an intermediate circular support and a free inner edge.
23. S. K. JANG and C. W. BERT 1989 *Journal of Sound Vibration* **130**, 342–346. Free vibration of stepped beams: exact and numerical solutions.
24. R. D. BLEVINS 1979 *Formulas for Natural Frequency and Mode Shape*. New York: Van Nostrand Reinhold Company.
25. P. A. A. LAURA and P. L. VERNIERE DE IRASSAR 1981 *Applied Acoustics* **14**, 93–99. Vibrations of a beam fixed at one end and carrying a guided mass at the other.
26. K. S. GRANHAM 1996 *Schaum's Outline of Theory and Problems of Mechanical Vibrations*. New York: McGraw-Hill.
27. E. A. BAMBILL and P. A. A. LAURA 1989 *Journal of Sound Vibration* **130**, 167–170. Application of the Rayleigh–Schmidt method when the boundary conditions contain the eigenvalues of the problem.
28. R. P. GOEL 1976 *Journal of Sound Vibration* **47**, 9–14. Free vibrations of a beam–mass system with elastically restrained ends.
29. L. S. SRINATH and Y. C. DAS 1967 *Journal of Applied Mechanics* **34**, 784–785. Vibrations of beams carrying mass.